NeuroImage 310 (2025) 121121



Contents lists available at ScienceDirect

NeuroImage

journal homepage: www.elsevier.com/locate/ynimg





Anatomical abnormalities suggest a compensatory role of the cerebellum in early Parkinson's disease

Juyoung Jenna Yun [a,b], Anastasia Gailly de Taurines [a,b], Yen F Tai [b,c], Shlomi Haar [a,b,*]

[a] UK Dementia Research Institute – Care Research and Technology Centre, Imperial College London, London, United Kingdom
[b] Department of Brain Sciences, Imperial College London, London, United Kingdom
[c] Department of Neurology, Charing Cross Hospital, London, United Kingdom

ARTICLE INFO

Keywords:
Parkinson's disease
Cerebellum
Neuroimaging
Anatomy
Atrophy

ABSTRACT

Brain atrophy is detected in early Parkinson's disease (PD) and accelerates over the first few years post-diagnosis. This was captured by multiple cross-sectional studies and a few longitudinal studies in early PD. Yet only a longitudinal study with a control group can capture accelerated atrophy in early PD and differentiate it from healthy ageing. Accordingly, we performed a multicohort longitudinal analysis between PD and healthy ageing, examining subcortical regions implicated in PD pathology, including the basal ganglia, thalamus, corpus callosum (CC), and cerebellum. Longitudinal volumetric analysis was performed on 56 early PD patients and 53 matched controls, with scans collected 2–3 years apart. At baseline, the PD group showed a greater volume in the pallidum, thalamus, and cerebellar white matter (WM), suggesting potential compensatory mechanisms in prodromal and early PD. After 2–3 years, accelerated atrophy in PD was observed in the putamen and cerebellar WM. Interestingly, healthy controls – but not PD patients – demonstrated a significant decline in Total Intracranial Volume (TIV), and atrophy in the thalamus and mid-CC. Between-group analysis revealed more severe atrophy in the right striatum and cerebellar WM in PD, and in the mid-posterior CC in controls. Using CEREbellum Segmentation (CERES) for lobule segmentation on the longitudinal PD cohort, we found a significant decline in the WM of non-motor regions in the cerebellum, specifically Crus I and lobule IX. Our results highlight an initial increase in cerebellar WM volume during prodromal PD, followed by significant degeneration over the first few years post-diagnosis.

1. Introduction

Extensive research indicates that Parkinson's disease (PD) involves the degeneration of the basal ganglia (BG), particularly the dopaminergic neurons within the Substantia Nigra (SN), leading to the hallmark motor deficits observed in the disease (Marsden, 1990). The neurodegenerative process in PD is characterised by a critical loss of striatal volume, with atrophy in the caudate and putamen, which are integral to the cortico-basal ganglia-thalamo-cortical loop involved in motor control (Pitcher et al., 2012). The atrophy and disrupted neuronal activity within these regions undermine the equilibrium between the direct and indirect motor pathways, resulting in the movement impairments characteristic of PD (Szewczyk-Krolikowski et al., 2014).

Notably, by the time motor symptoms become apparent in PD patients, over 50 % of the dopaminergic neurons in the SN have been lost (Marsden, 1990). This neuronal loss correlates with the deterioration of the basal ganglia's functionality, as evidenced by reduced resting functional connectivity and the subsequent decline in cognitive abilities as the disease progresses (Szewczyk-Krolikowski et al., 2014; Lopes et al., 2016). Furthermore, the striatum's volume has been positively associated with 'motor reserve', a concept describing the capacity to counteract motor decline by adapting relevant neural networks, highlighting its significance in the early stages of PD (Jeong et al., 2022; Hoenig et al., 2023).

In contrast to the decades' long focus on the BG itself, recent studies started to shed light on the potential compensatory role of the cortex (Johansson et al., 2024) and the cerebellum (Simioni et al., 2016; Li, Le and Jankovic, 2023), and their connections with the BG in the cerebello-thalamo-cortical loop (Abulikemu et al., 2023). Recent work, including a cross-sectional study by Kerestes et al. (2023), identified abnormal cerebellar volumes in PD patients compared to a control group. This study underlined the potential link between early-stage PD

* Corresponding author.
E-mail address: s.haar@imperial.ac.uk (S. Haar).

https://doi.org/10.1016/j.neuroimage.2025.121121
Received 29 August 2024; Received in revised form 3 March 2025; Accepted 4 March 2025
Available online 5 March 2025
1053-8119/© 2025 The Authors. Published by Elsevier Inc. This is an open access article under the CC BY license (http://creativecommons.org/licenses/by/4.0/).

and dysregulation in the anterior cerebellum and alterations in the posterior non-motor lobes in the later stages of the disease.

Therefore, our study seeks to investigate the volumetric changes within these key brain structures in early PD, over the first 2–3 years post-diagnosis, utilising T1-weighted MRI data. This longitudinal perspective is crucial to identify compensatory mechanisms in prodromal and early PD and to reconcile the diverse findings of previous studies. By analysing both the grey and white matter alterations over time, we aim to provide a clearer picture of PD's progression, which could contribute to a better understanding of PD.

2. Methods

2.1. Participants

In this study, we analysed MRI scans for a cohort of people living with PD from the Parkinson's Progression Markers Initiative (PPMI; see https://www.ppmi-info.org), and the cohort of healthy aging from the Open Access Series of Imaging Series 3 (OASIS-3; see https://sites.wustl.edu/oasisbrains/home/oasis-3/).

PPMI is a muti-centre observational study of clinical and neuroimaging progression markers of PD conducted since 2010. The study design and protocol are available online (https://www.ppmi-info.org/study-design). The study and the data collection have been performed in accordance with the Declaration of Helsinki and were approved by the institutional review board or local ethics committee at each of the participating sites (https://www.ppmi-info.org/about-ppmi/ppmi-clinical-sites). All PPMI participants provided written informed consent.

OASIS-3 is a longitudinal multimodal neuroimaging, clinical, and cognitive dataset for normal aging and Alzheimer's Disease. It is a retrospective compilation of data for 1378 participants that were collected across several ongoing projects through the WUSTL Knight ADRC over the course of 30 years. Participants consented to the use of their data by the scientific community and data sharing terms have been approved by the Washington University Human Research Protection Office.

As the PPMI dataset did not provide a sufficient age-and-sex-matched healthy controls, we obtained these controls from the OASIS-3 dataset. From the PPMI, we acquired clinical and MRI data of PD patients, who have had at least two scans 2–3 years apart, with motor symptoms such as tremor or bradykinesia, scanned within two years from diagnosis, and medication-naïve prior to baseline scan. The patients were all medicated by the time the second scans were acquired. Exclusions included any significant cognitive impairments or comorbidities that could affect the MRI scan. Two cognitive rating scores were used when selecting participants: the United Parkinson's Disease Rating Scale (UPDRS) and the Montreal Cognitive Assessment (MoCA). Here we included only participants who had an initial score for the UDPRS-part I cognitive impairment of 0, no neuropathological conditions like Alzheimer's Disease or Chronic Traumatic Encephalopathy, and a MoCA score above 26. This is to ensure participants exhibited no significant cognitive impairment which may confound our results. Individuals with a score below 26 have previously been found to display difficulties completing cognitive and motor tasks, despite intact motor function (Nazem et al., 2009). In addition to controlling for the confounding factors, we also minimised motion artefacts by checking for the MRI quality documentation provided by the PPMI dataset. Here, we disregarded participants with poor or "nan" scores. This was cross-analysed through manual inspection of the MRI scans.

The control cohort was derived from the OASIS-3 dataset, which comprised cognitively normal adults aged between 42 and 95 years, without a biological parental history of Alzheimer's disease, and who had undergone regular cognitive assessments over 15 years. Any indications of cognitive or functional decline reported by cohabitants or comorbidities found in MRI scans resulted in exclusion from our longitudinal dataset.

After the initial selection, demographic outliers were eliminated if they exceeded 3 standard deviations (SD) from the mean.

2.2. Imaging acquisition

T1 MRIs were selected for matching dimensions and voxel sizes, ensuring a well-regulated comparison. The field strength, scanner manufacturer, echo time (TE) and repetition time (TR) were all matched between the two datasets (Table S1). While there were differences in TE and TR times, those were not statistically significant ($p = 0.27$ for TE and $p = 0.054$ for TR). For all scans in both cohorts, the T_1-weighted MRI data consisted of 176 slices with a matrix size of 256 × 256 and voxel sizes of 1.0 × 1.0 × 1.0 mm in plane resolution. Participants who did not meet these parameters were excluded from the study. The effect of site differences was not assessed due to the lack of disclosed information.

2.3. T_1–weighted MRI data preprocessing

MRI data were preprocessed with the Freesurfer software package 7.3.2 (Fischl, 2012). This includes the removal of non-brain tissue, and segmentation of subcortical grey and white matter based on image intensity. Individual brains were registered to an atlas parcellating the subcortical regions of interest (ROIs) using the Destrieux anatomical atlas (Destrieux et al., 2010). Based on our interest in the Cortico-basal ganglia-thalamo-cortical (CBTC) and the cerebello-thalamo-cortical (CTC) circuits, the subcortical ROIs analysed were: Caudate, Putamen, Pallidum, Thalamus, and Cerebellar Grey and White Matter (Fig. 1). Other white matter regions, such as cerebral white matter and corpus callosum (CC), were included due to previous findings of their involvement in PD (Taylor et al., 2018).

2.4. Segmentation of cerebellar white and grey matter

For further parcellation of the cerebellum, a multi-atlas segmentation tool, CEREbellum Segmentation (CERES), was used to automatically parcellate the cerebellum lobule (Romero et al., 2017). CERES employs an optimised patch-based algorithm and demonstrates superior accuracy and execution time when parcellating the cerebellum compared to other pipelines (Romero et al., 2017). CERES includes the white and grey matter volumes of 12 cerebellar lobules, along with cortical thickness measurements (Fig. 1).

2.5. Statistical analysis

Regional volume was selected as the primary measure for assessing structural changes. For within and between-subject comparisons, the volumetric regional measures were normalised by the Total Intracranial Volume (TIV) (Whitwell et al., 2001; Haar et al., 2016).

To assess volumetric changes in PD patients and healthy controls over time, we utilised Shapiro-Wilk tests to confirm non-normal data distribution, leading to the application of non-parametric Wilcoxon Signed-Rank and Mann-Whitney U tests for within-group and between-group comparisons, respectively. Python and Prism facilitated these analyses, with False Discovery Rate (FDR) correction used for multiple comparisons.

3. Results

Following screening, our cohort consisted of 56 PD patients (35 men and 21 women, aged 62.44 ± 9.62 years, mean ± SD) and 53 controls (32 men and 21 women, aged 64.77 ± 7.47 years, mean ± SD). There was no significant difference in age and gender between the two groups (Table 1). The scan year difference within the control group (2.54 ± 0.68 years, mean ± SD) was significantly greater than in the PD group (2.09 ± 0.29 years, mean ± SD). The handedness ratios differences

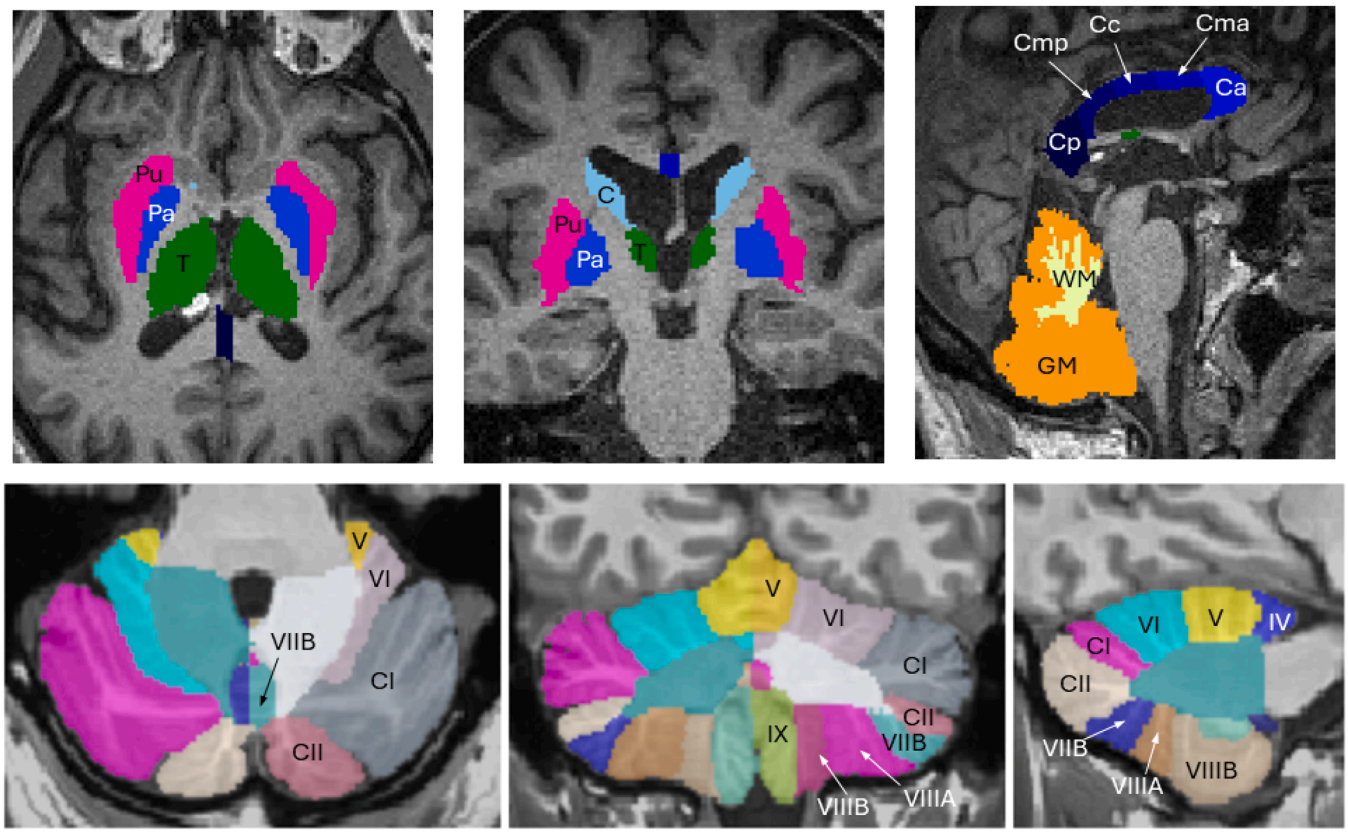


Fig. 1. Anatomical regions highlighted on a T1-weighted MRI scan. The upper panel includes the subcortical ROIs from the Freesurfer Destrieux anatomical atlas: ***T*** = thalamus, **Pu** = putamen, **Pa** = pallidum, **C** = caudate, **WM** = cerebellum white matter, **GM** = cerebellum grey matter, **Cp** = posterior CC, **Cmp** = mid-posterior CC, **Cc** = central CC, **Cma** = mid-anterior CC, and **Ca** = anterior CC. The lower panel displays the cerebellum segmentation based on the CERES atlas.

Table 1
Demographic and Clinical Data of the PD patients and healthy controls. Age, Disease duration, Scan Difference, UPDRS III, IV, and MoCA scores are calculated in mean ± SD, whereas Hoehn and Yahr (H-Y) PD functional disability scale and UPDRS-I scores are calculated in median (range). The UPDRS III Total Score Post-2/3 years were measured during the ON medication state.

	Control (n = 53)	PD (n = 56)	t/x^2	p-value
Gender, M/F	32/21	35/21	0.00	0.97
Age, year	64.77 ± 7.47	62.44 ± 9.62	1.40	0.16
Handedness, R/L/B	47/5/1	47/6/3	1.01	0.60
Disease duration, years	–	2.28 ± 0.80	–	–
Scan Difference, years	2.54 ± 0.68	2.09 ± 0.29	4.55	1.47e-05
Dominant PD side, R/L	–	22/34		
H-Y stage, Baseline	–	1 (1–2)	–	–
H-Y stage, Post-2/3 years	–	2 (1–3)	–	–
UPDRS-I, Cognitive Score	–	0 (0–1)	–	–
UPDRS-III, Total Score (Baseline)	–	21.6 ± 8.94	–	–
UPDRS-III, Total Score (Post-2/3 years)		24.8 ± 11.9	–	–
UPDRS-IV, Motor Complications	–	0.55 ± 1.93	–	–
MoCA	–	27.3 ± 1.93	–	–

between the two groups were insignificant. Table 1 summarises the demographic and clinical characteristics of the participants.

3.1. Baseline comparison

The region-specific volumetric comparisons in this study were done after normalising for TIV. TIV itself showed no significant differences between PD patients and controls, in the non-parametric Mann-Whitney U test ($z = 0.10$, $p = 0.92$), used due to non-normal distribution after testing the normality using Shapiro-Wilk test (Fig. 2). Subsequent analysis of specific ROIs normalised against TIV revealed significant volumetric differences in the bilateral pallidum, thalamus, and cerebellar white matter (q(FDR corrected significance) < 0.05), all showing higher volume in PD (Fig. 2). In the cerebellum and thalamus, the left hemisphere had a greater difference than the right. Anterior CC also depicted a marginal difference, whereby the patient group was higher than the control group ($p = 0.02$) though this significance did not survive FDR correction.

3.2. Longitudinal volumetric changes after 2/3 years

To examine longitudinal changes over 2 to 3 years, we performed a one-sided Wilcoxon signed-rank test. The control group displayed a significant decline in TIV ($q = 0.013$) but not the PD group ($q = 0.56$). While TIV decline showed no significant difference between PD patients and controls ($z = -2.23$, $q = 0.074$), there was a trend of less severe decline in PD. Specific brain regions (Fig. 3 and Table S2) highlighted differential patterns of volumetric change (normalised for TIV). In healthy controls, notable decreases were observed in the thalamus ($q = 0.007$) and mid-CC ($q < 0.001$), suggesting these areas are particularly susceptible to changes associated with normal ageing. Conversely, the

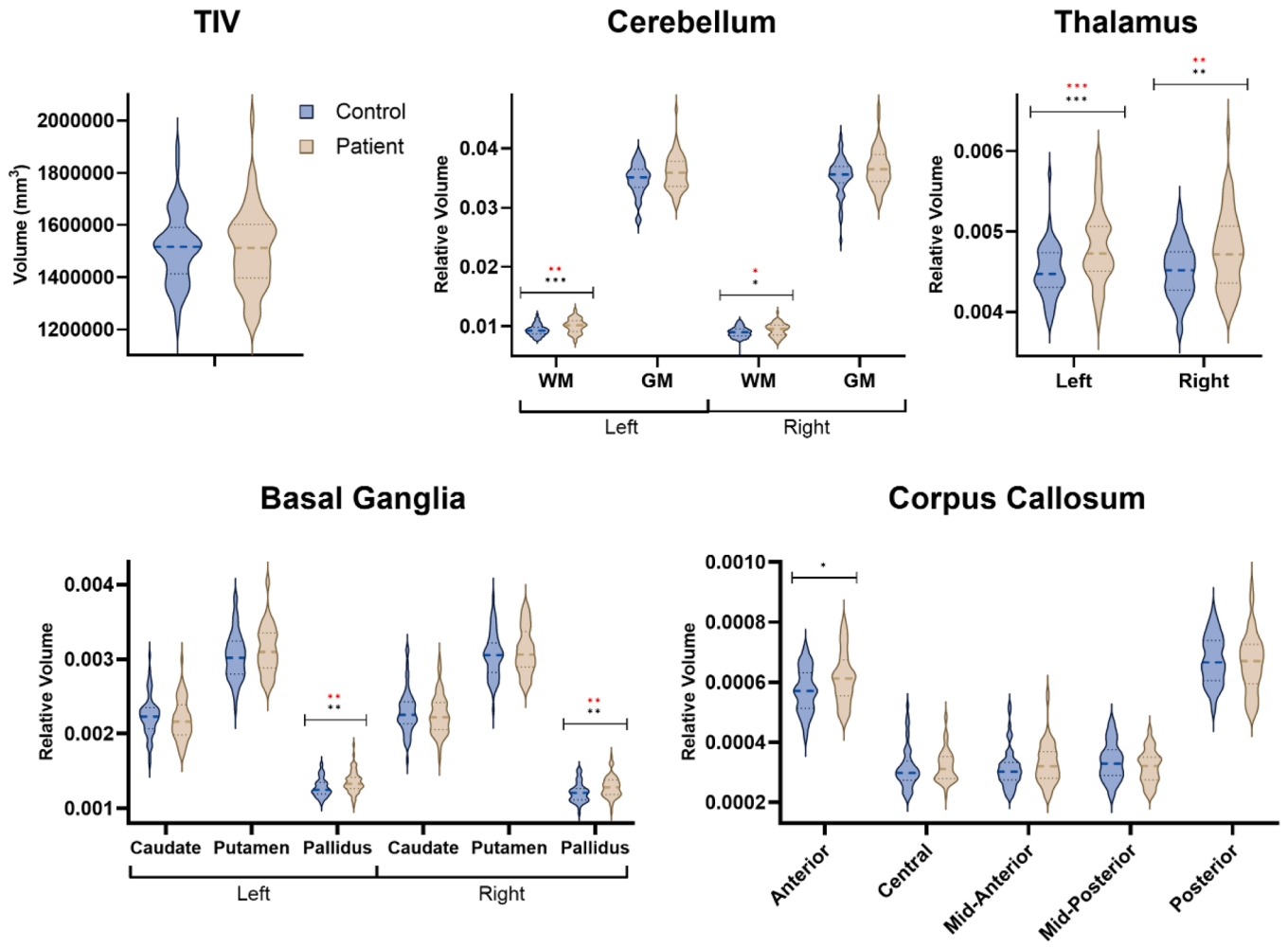


Fig. 2. Baseline Comparison of TIV and Relative Volume in the Regions of Interest. The regional volume is presented as a portion of the TIV. Between-group differences were tested using the Mann-Whitney U test and FDR multiple comparisons correction. Significance levels are plotted by uncorrected p-values (black asterisk) and FDR-corrected q-values (red asterisk). *: values<0.05, **: values<0.01, ***: values<0.001. Cerebellum is labelled as: WM = white matter, GM = grey matter.

PD group demonstrated a volumetric decrease in the putamen ($p < 0.05$, $q = 0.06$) and a most significant decrease in the cerebellar white matter ($p = 0.002$, $q = 0.03$). Comparative analyses between groups were done using the Mann-Whitney U test. Multiple regions reported uncorrected significant differences including the right striatum and cerebellar white matter ($p < 0.05$), but the only ROI showing significant group difference after correcting for multiple comparisons was the mid-posterior CC ($q = 0.007$).

3.3. Relative volume comparison in the cerebellum in pd

To better assess group differences in the observed cerebellar decline, we used the CERES pipeline to parcellate the cerebellar volume into 12 lobules. The white matter in PD Crus I and lobule IX showed the most significant decline, with Crus I showing a notable volume decrease in both cerebellar hemispheres (left: $q = 0.02$, right: $q < 0.001$) and lobule IX displaying a significant decline in the left hemisphere ($q = 0.02$) while the decline in right lobule IX did not survive FDR correction ($p < 0.02$, $q = 0.088$). This lateralization is in agreement with the one observed in the striatum and might be due to the left dominance PD symptoms in this cohort. Additional cerebellar regions exhibited marginal significance that did not withstand rigorous multiple comparison corrections (Fig. 4 and Tables S3 and S4). In contrast, the control group shared a minimal significance in right lobule VI ($q = 0.044$) and none in other lobules (Tables S5 and S6).

4. Discussion

In this study, we explored volumetric changes in subcortical grey and white matter across a 2 to 3-year interval in early PD patients alongside an age-matched healthy control cohort. The longitudinal approach and the inclusion of healthy controls, matched for confounding factors, allowed a focused longitudinal examination of regional volumetric alterations. Our findings underline the crucial role of the cerebellum in early PD progression. We showed that during baseline, shortly after PD diagnosis, patients had increased volume in cerebellar white matter, but over the following 2–3 years, this area showed the most significant decrease in volume. These results suggest a potential compensatory role of the cerebellum in prodromal and early PD which changes around diagnostic and symptoms appearance. We further delved into cerebellar lobule segmentation and localised this volume decrease in Crus I, which was previously suggested to be a hub of the functional cerebellar connectome (Chen et al., 2022).

While there were no significant differences in the Total Intracranial Volume between the early PD patients and matching controls at baseline, PD patients displayed a higher volume in multiple subcortical regions, including the cerebellar white matter, pallidum, and thalamus (Whone et al., 2003). This may indicate the initial compensatory

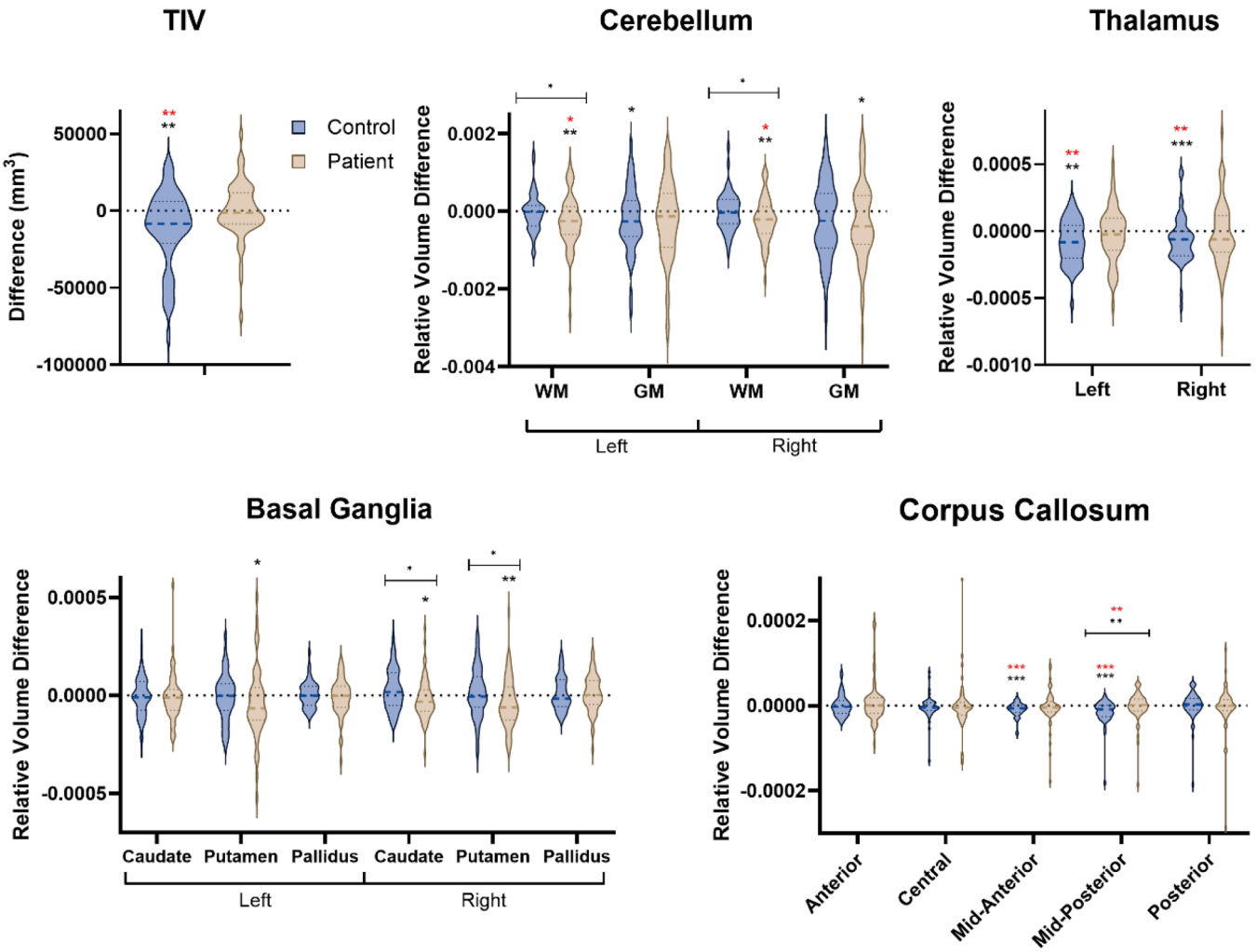


Fig. 3. Change in the TIV and Relative Volume of the Selected Regions after 2/3 Years. The regional volume is presented as a portion of the TIV. Between-group differences were tested using the Mann-Whitney U test and FDR multiple comparisons correction. Significance levels are illustrated by uncorrected p-value (black asterisk) and corrected q-value (red asterisk). *: values<0.05, **: values<0.01, ***: values<0.001. Cerebellum is labelled as: WM = white matter, GM = grey matter.

mechanism in prodromal and early PD (Brotchie and Fitzer-Attas, 2009; Blesa et al., 2017). A few previous studies reported differences in pallidum volume between control and PD groups, though with no statistical significance (Yang et al., 2024). While some previous studies found no detectable regional atrophy differences in the thalamus of PD patients and controls (McKeown et al., 2008; Ibarretxe-Bilbao et al., 2012; Tessa et al., 2014), others reported an increased thalamic volume in early PD patients (Jia et al., 2015). A more recent study looking into all volume, thickness, and surface area of the thalamus highlighted an overall bigger thalamus in early PD patients (Kerestes et al., 2023). The significantly higher cerebellar white matter volume in PD patients is consistent with a recent observation of a higher anterior cerebellar volume in the initial stage of PD compared to controls. It is also in line with the proposed hyperactivation of the cerebellothalamic pathway explained by basal ganglia dysfunction (Helmich et al., 2011). Recent studies demonstrate a growing interest in understanding the reciprocal interaction between the cerebellum and basal ganglia (Bostan and Strick, 2018). An anatomical tracing study underlined both cerebellum-striatum and subthalamic nucleus-cerebellum networks via the thalamus and pontine nucleus, respectively (Washburn et al., 2024). Our findings in increased cerebellar white matter volume in early PD patients may suggest basal ganglia-mediated hyperactivation, which is shown to be relevant in understanding PD tremors as well (Helmich et al., 2011).

Our longitudinal analysis over a 2–3-year period suggests that the TIV decreases as part of healthy ageing, though this decay was significant only within the control group, but not in the PD group. Yet, the difference in the decay between the groups lacked significance. This is consistent with earlier findings of increased TIV in PD (Krabbe et al., 2005). In the studied ROIs, the overall trend was of volumetric decay but while some regions showed more severe decay in PD others showed more severe decay in the control group. Healthy controls demonstrated the greatest reduction in the mid-CC and thalamus, whereas the PD patients had the biggest reduction in the volume of the cerebellar white matter. The mid-posterior CC was identified as a region with the greatest difference between the groups, showing greater decay in healthy controls. A recent longitudinal study in PD reported no structural change in the CC in a 21-month follow-up (Wu et al., 2020); we also found no change in PD but show that this is in contrast to a significant change in healthy ageing. This highlights the importance of healthy control comparison in longitudinal patient studies.

In PD patients, the biggest change was observed in the cerebellar white matter, which is consistent with the pathological α-synuclein aggregates found in the lobular white matter tracts (Seidel et al., 2017). One of the main hypotheses revolving around the selective neuronal vulnerability observed in PD is based on α-synuclein pathology, where insoluble synuclein aggregation can disseminate along neural pathways in a prion-like mechanism. Previously, studies have shown that Lewy bodies formed in the Substantia Nigra positively correlates with the

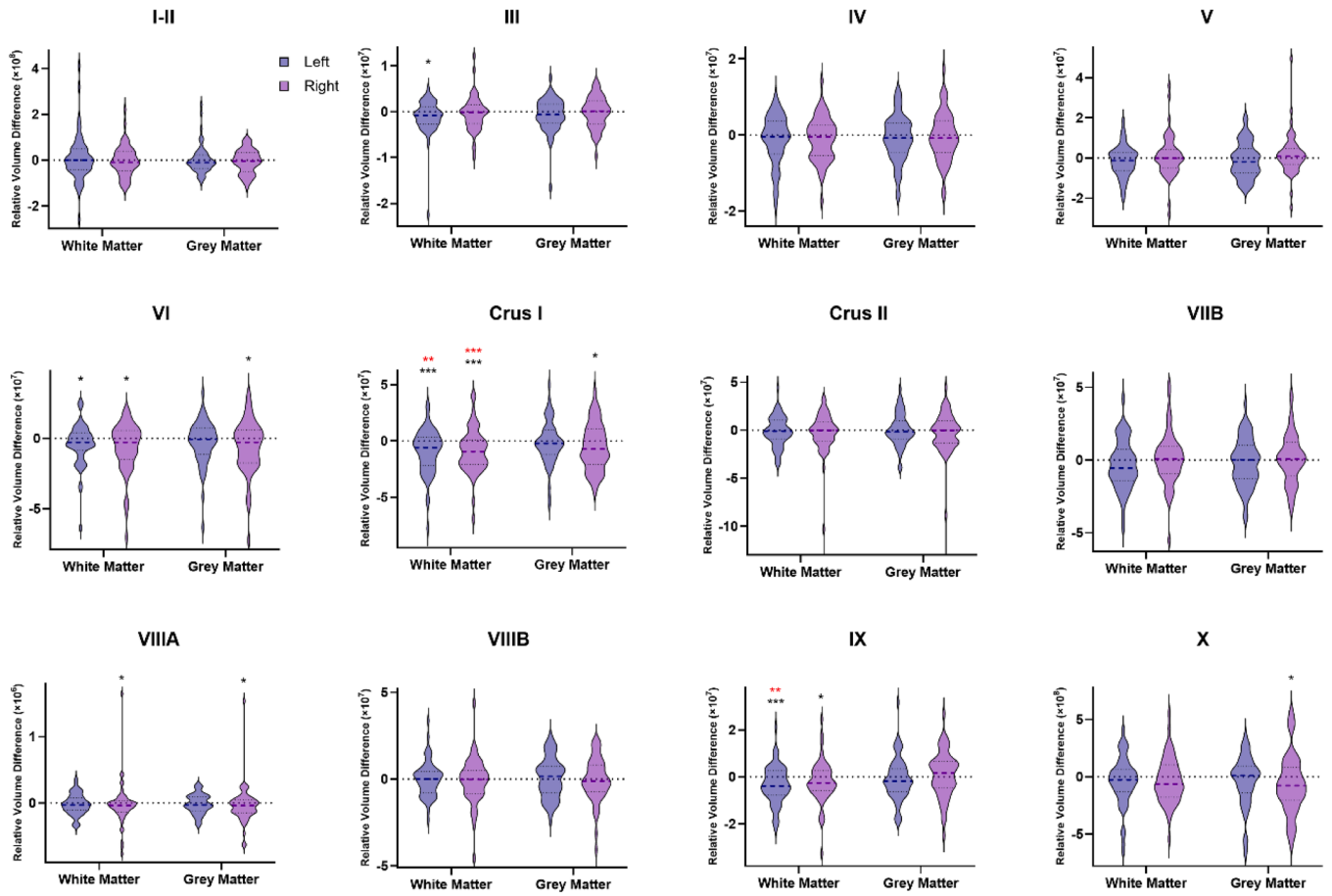


Fig. 4. Change in Relative Volume in the Cerebellum of PD Patient after 2/3 Years. The regional volume was normalised to the TIV. Within-group differences were tested using the Wilcoxon test and FDR multiple comparisons. Significance levels were represented by uncorrected p-values (black asterisk) and corrected q-values (red asterisk). *: values<0.05, **: values<0.01, ***: values<0.001.

symptom severity (Hartmann, 2004). The presence of α-synuclein aggregates in the cerebellum along with our findings suggests an importance in investigating early pathology in the cerebellum.

Kerestes et al. (2023) also observed notable changes in the cerebellar volume based on HY score increment. Interestingly, the cerebellum is considered to be one of the brain areas which undergoes the slowest neurodegeneration (Liang and Carlson, 2020) and to play a role in compensatory mechanism in early PD (Simioni, Dagher and Fellows, 2016). The fast WM volumetric decay presented here might capture the transition from its compensatory role to its neurodegeneration towards distinct cerebellar atrophy in advanced PD (O'Callaghan et al., 2016).

Looking deeper into the cerebellar volumetric decay, our results suggest that bilateral Crus I and the left IX lobule have the greatest volumetric loss in PD after a 2/3-year follow-up. Multiple studies observed degeneration in Crus I in advanced PD patients (O'Callaghan et al., 2016; Erro et al., 2020) and one classified PD patients from matched controls based on cerebellum Crus I grey matter degeneration with 95 % accuracy (Zeng et al., 2017). Ongoing research continues to uncover cerebellar macrostructural changes in PD relative to cognitive impairments. A recent study using the same segmentation tool as ours, CERES, found a strong association between the cerebellum and cognitive function (Bègue et al., 2023). In particular, Crus I showed a positive association with working memory. Hence, the decreased Crus I WM volume in our findings may explain the developing non-motor symptoms in PD patients. Moreover, enhanced Crus I activity and its increased connectivity with the putamen are positively correlated with cognitive assessments like MoCA, indicating the region's role in cognitive impairments in PD (Shen et al., 2020; Solstrand Dahlberg et al., 2020). This is further supported by the recent findings by Kerestes et al. (2023), which underlined the association between cognitive performance and the decline in cerebellar volume, suggesting the critical link between the cerebellum and cognitive function in PD. Additionally, the abnormal changes found in Crus I may link with other non-motor symptoms like depression, which is prevalent in early PD patients (Aarsland et al., 2012). In fact, a recent study on melancholia, one of the subtypes of depression, underlined a few lobules including Crus I as a key finding in understanding facial expressiveness (Mosley et al., 2024).

There are limited reported findings on lobule IX in PD pathology, though one study observed a difference in lobule IX between PD and healthy controls (Gardoni et al., 2023). The change in lobule IX does not seem to have a strict relationship with either motor or non-motor symptomatology. Rather, the current literature suggests a more intricate participation in both. For instance, one study found a strong correlation between depression, anxiety, and IX atrophy (Ma et al., 2018). This is further explained by the involvement of the cerebellum in the cortico-limbic network, regulating the negative emotion processing (Adamaszek et al., 2017). Some also suggest an involvement of lobule IX in visuospatial impairment in PD (Lawn and ffytche, 2021; Yin et al., 2021). In contrast, a few studies suggest an increased IX activity in dopamine-resistant PD tremor (Dirkx et al., 2019). This is particularly relevant as the cerebellum consists mainly of non-dopaminergic transmitters (Zhong et al., 2022). Similarly, Lopez and colleagues emphasised the relevance of XI in predicting resting tremors in PD patients (Lopez et al., 2020). Nonetheless, a further investigation of the involvement of lobule IX in PD symptomology is required.

While our study presents the most complete analysis of anatomical

changes in PD to date, combining cross-sectional and longitudinal design, it was subject to several known limitations. First, our results are based on Freesurfer segmentation, which while considered state-of-the-art, when comparing pathological conditions with controls some issues were found in some of its previous versions (Filip et al., 2022). Our study implemented the recently updated Freesurfer version 7.3.2, which should be more robust, but its replicability and reproducibility have not yet been externally tested and reported. Second, the MRI data for the PD patients and controls were obtained from different multisite datasets. Though we controlled for TE and TR variability, there are likely additional confounding factors. There was also high variability in voxel dimensions within the same dataset that needed to be controlled for. Lastly, in the dataset, there was no clinical score off medication at the time of the second scan. The lack of longitudinal clinical score limits the clinical interpretation of the imaging data.

In conclusion, anatomical MRI data of PD patients and matching controls at baseline and 2/3-year follow-up, demonstrate significantly different volumetric decay between the groups. Our approach revealed that the cerebellar WM showed significantly increased atrophy in PD relative to healthy ageing. This was driven by atrophy in cerebellar Crus I and IX white matter in early PD pathology. Furthermore, our analysis enabled us to explore potential compensatory increases in volume in the thalamus and mid-CC in early PD, relative to changes observed in healthy ageing. Future data collection efforts over longer periods with shorter intervals will enhance our understanding of structural changes during PD progression. Future work should aim to comprehensively identify morphological brain changes that occur before the onset of PD symptoms to improve the understanding of PD pathology.

5. Data and code availability statement

The data used is from publicly available datasets: the Parkinson's Progression Markers Initiative (PPMI, https://www.ppmi-info.org), and the Open Access Series of Imaging Series 3 (OASIS-3, https://sites.wustl.edu/oasisbrains/home/oasis-3).

CRediT authorship contribution statement

Juyoung Jenna Yun: Writing – review & editing, Writing – original draft, Visualization, Methodology, Formal analysis. **Anastasia Gailly de Taurines:** Writing – review & editing, Formal analysis. **Yen F Tai:** Writing – review & editing, Formal analysis. **Shlomi Haar:** Writing – review & editing, Visualization, Validation, Supervision, Methodology, Formal analysis, Conceptualization.

Declaration of competing interest

The authors declare that they have no known competing financial interests or personal relationships that could have appeared to influence the work reported in this paper.

Acknowledgements

The study was supported by the UK Dementia Research Institute, Care Research & Technology Centre and SH's Edmond and Lily Safra Fellowship. The PD data used in the preparation of this article were obtained from the Parkinson's Progression Markers Initiative (PPMI) database (https://www.ppmi-info.org). PPMI – a public-private partnership – is funded by The Michael J. Fox Foundation for Parkinson's Research and funding partners listed here https://www.ppmi-info.org/about-ppmi/who-we-are/studysponsors. The HC data were obtained from the Open Access Series of Imaging Series 3 (OASIS-3, https://sites.wustl.edu/oasisbrains/home/oasis-3).

Supplementary materials

Supplementary material associated with this article can be found, in the online version, at doi:10.1016/j.neuroimage.2025.121121.

References

Aarsland, D., et al., 2012. Depression in Parkinson disease—Epidemiology, mechanisms and management'. Nat. Reviews Neurology 8 (1), 35–47. https://doi.org/10.1038/nrneurol.2011.189.

Abulikemu, S., Tai, Y.F., Haar, S., 2023. Modulatory Effect of Levodopa on the Basal Ganglia-Cerebellum Connectivity in Parkinson's Disease'. bioRxiv. https://doi.org/10.1101/2023.01.16.524229, p. 2023.01.16.524229.

Adamaszek, M., et al., 2017. Consensus paper: cerebellum and emotion. The Cerebellum 16 (2), 552–576. https://doi.org/10.1007/s12311-016-0815-8.

Bègue, I., et al., 2023. The cerebellum and cognitive function: anatomical evidence from a transdiagnostic sample. The Cerebellum. https://doi.org/10.1007/s12311-023-01645-y.

Blesa, J., et al., 2017. Compensatory mechanisms in Parkinson's disease: circuits adaptations and role in disease modification. Exp. Neurol. 298, 148–161. https://doi.org/10.1016/j.expneurol.2017.10.002.

Bostan, A.C., Strick, P.L., 2018. The basal ganglia and the cerebellum: nodes in an integrated network. Nat. Rev. Neurosci. 19 (6), 338–350. https://doi.org/10.1038/s41583-018-0002-7.

Brotchie, J., Fitzer-Attas, C., 2009. Mechanisms compensating for dopamine loss in early Parkinson disease. Neurology. 72 (7_supplement_2). https://doi.org/10.1212/WNL.0b013e318198e0e9.

Chen, Z., et al., 2022. Functional connectome of human cerebellum. Neuroimage 251, 119015. https://doi.org/10.1016/j.neuroimage.2022.119015.

Destrieux, C., et al., 2010. Automatic parcellation of human cortical gyri and sulci using standard anatomical nomenclature. NeuroImage 53 (1), 1–15. https://doi.org/10.1016/j.neuroimage.2010.06.010.

Dirkx, M.F., et al., 2019. Cerebral differences between dopamine-resistant and dopamine-responsive Parkinson's tremor. Brain 142 (10), 3144–3157. https://doi.org/10.1093/brain/awz261.

Erro, R., et al., 2020. Subcortical atrophy and perfusion patterns in Parkinson disease and multiple system atrophy. Parkinsonism. Relat. Disord. 72, 49–55. https://doi.org/10.1016/j.parkreldis.2020.02.009.

Filip, P., et al., 2022. Different FreeSurfer versions might generate different statistical outcomes in case–control comparison studies. Neuroradiology. 64 (4), 765–773. https://doi.org/10.1007/s00234-021-02862-0.

Fischl, B., 2012. FreeSurfer. Neuroimage 62 (2), 774–781. https://doi.org/10.1016/j.neuroimage.2012.01.021.

Gardoni, A., et al., 2023. Cerebellar alterations in Parkinson's disease with postural instability and gait disorders. J. Neurol. 270 (3), 1735–1744. https://doi.org/10.1007/s00415-022-11531-y.

Haar, S., et al., 2016. Anatomical abnormalities in autism? Cerebral Cortex 26 (4), 1440–1452. https://doi.org/10.1093/cercor/bhu242.

Hartmann, A., 2004. Postmortem studies in Parkinson's disease. Dialogues. Clin. Neurosci. 6 (3), 281–293.

Helmich, R.C., et al., 2011. Pallidal dysfunction drives a cerebellothalamic circuit into Parkinson tremor. Ann. Neurol. 69 (2), 269–281. https://doi.org/10.1002/ana.22361.

Hoenig, M.C., et al., 2023. The concept of motor reserve in parkinson's disease: new wine in old bottles? Mov. Disord. 38 (1), 16–20. https://doi.org/10.1002/mds.29266.

Ibarretxe-Bilbao, N., et al., 2012. Progression of cortical thinning in early Parkinson's disease. Movement Disord. 27 (14), 1746–1753. https://doi.org/10.1002/mds.25240.

Jeong, S.H., et al., 2022. Local striatal volume and motor reserve in drug-naïve Parkinson's disease. npj Parkinsons Dis. 8 (1), 1–9. https://doi.org/10.1038/s41531-022-00429-1.

Jia, X., et al., 2015. Longitudinal study of gray matter changes in Parkinson Disease. AJNR: Am. J. Neuroradiol. 36 (12), 2219–2226. https://doi.org/10.3174/ajnr.A4447.

Johansson, M.E., et al., 2024. Clinical severity in Parkinson's disease is determined by decline in cortical compensation. Brain 147 (3), 871–886. https://doi.org/10.1093/brain/awad325.

Kerestes, R., et al., 2023. Cerebellar volume and disease staging in Parkinson's disease: an ENIGMA-PD study. Movement Disord. 38 (12), 2269–2281. https://doi.org/10.1002/mds.29611.

Krabbe, K., et al., 2005. Increased intracranial volume in Parkinson's disease. J. Neurol. Sci. 239 (1), 45–52. https://doi.org/10.1016/j.jns.2005.07.013.

Lawn, T., ffytche, D., 2021. Cerebellar correlates of visual hallucinations in Parkinson's disease and Charles Bonnet Syndrome. Cortex 135, 311–325. https://doi.org/10.1016/j.cortex.2020.10.024.

Li, T., Le, W., Jankovic, J., 2023. Linking the cerebellum to Parkinson disease: an update. Nat. Rev. Neurol. 19 (11), 645–654. https://doi.org/10.1038/s41582-023-00874-3.

Liang, K.J., Carlson, E.S., 2020. Resistance, vulnerability and resilience: a review of the cognitive cerebellum in aging and neurodegenerative diseases. Neurobiol. Learn. Mem. 170, 106981. https://doi.org/10.1016/j.nlm.2019.01.004.

Lopes, R., et al., 2016. Cognitive phenotypes in parkinson's disease differ in terms of brain-network organization and connectivity. Hum. Brain Mapp. 38 (3), 1604–1621. https://doi.org/10.1002/hbm.23474.

Lopez, A.M., et al., 2020. Structural correlates of the sensorimotor cerebellum in Parkinson's disease and essential tremor. Movement Disorders 35 (7), 1181–1188. https://doi.org/10.1002/mds.28044.
Ma, X., et al., 2018. Cerebellar atrophy in different subtypes of Parkinson's disease. J. Neurol. Sci. 392, 105–112. https://doi.org/10.1016/j.jns.2018.06.027.
Marsden, C.D., 1990. Parkinson's disease. Lancet 335 (8695), 948–952. https://doi.org/10.1016/0140-6736(90)91006-v.
McKeown, M.J., et al., 2008. Shape (but not volume) changes in the thalami in Parkinson disease. BMC. Neurol. 8, 8. https://doi.org/10.1186/1471-2377-8-8.
Mosley, P.E., et al., 2024. Markers of positive affect and brain state synchrony discriminate melancholic from non-melancholic depression using naturalistic stimuli. Mol. Psychiatry 1–13. https://doi.org/10.1038/s41380-024-02699-y.
Nazem, S., et al., 2009. Montreal Cognitive assessment performance in patients with Parkinson's Disease with "normal" global cognition according to mini-mental State examination score. J. Am. Geriatr. Soc. 57 (2), 304–308. https://doi.org/10.1111/j.1532-5415.2008.02096.x.
O'Callaghan, C., et al., 2016. Cerebellar atrophy in Parkinson's disease and its implication for network connectivity. Brain 139 (3), 845–855. https://doi.org/10.1093/brain/awv399.
Pitcher, T.L., et al., 2012. Reduced striatal volumes in Parkinson's disease: a magnetic resonance imaging study. Transl. Neurodegener. 1 (1), 17. https://doi.org/10.1186/2047-9158-1-17.
Romero, J.E., et al., 2017. CERES: a new cerebellum lobule segmentation method. Neuroimage 147, 916–924. https://doi.org/10.1016/j.neuroimage.2016.11.003.
Seidel, K., et al., 2017. Involvement of the cerebellum in Parkinson disease and dementia with lewy bodies. Ann. Neurol. 81 (6), 898–903. https://doi.org/10.1002/ana.24937.
Shen, B., et al., 2020. Altered putamen and cerebellum connectivity among different subtypes of Parkinson's disease. CNS. Neurosci. Ther. 26 (2), 207–214. https://doi.org/10.1111/cns.13259.
Simioni, A.C., Dagher, A., Fellows, L.K., 2016. Compensatory striatal–cerebellar connectivity in mild–moderate Parkinson's disease. NeuroImage: Clinical 10, 54–62. https://doi.org/10.1016/j.nicl.2015.11.005.
Solstrand Dahlberg, L., Lungu, O., Doyon, J., 2020. Cerebellar contribution to motor and non-motor functions in Parkinson's Disease: a meta-analysis of fMRI findings. Front. Neurol. 11. https://www.frontiersin.org/articles/10.3389/fneur.2020.00127 (Accessed: 15 August 2023).
Szewczyk-Krolikowski, K., et al., 2014. Functional connectivity in the basal ganglia network differentiates PD patients from controls. Neurology. 83 (3), 208. https://doi.org/10.1212/WNL.0000000000000592.
Taylor, K.I., et al., 2018. Progressive decline in gray and white matter integrity in de novo Parkinson's Disease: an analysis of longitudinal Parkinson progression markers initiative diffusion tensor imaging data. Front. Aging Neurosci. 10. https://www.frontiersin.org/articles/10.3389/fnagi.2018.00318 (Accessed: 15 August 2023).
Tessa, C., et al., 2014. Progression of brain atrophy in the early stages of Parkinson's disease: A longitudinal tensor-based morphometry study in de novo patients without cognitive impairment. Hum. Brain Mapp. 35 (8), 3932–3944. https://doi.org/10.1002/hbm.22449.
Washburn, S., et al., 2024. The cerebellum directly modulates the substantia nigra dopaminergic activity. Nat. Neurosci. 27 (3), 497–513. https://doi.org/10.1038/s41593-023-01560-9.
Whitwell, J.L., et al., 2001. Normalization of cerebral volumes by use of intracranial volume: implications for longitudinal quantitative MR imaging. AJNR: American Journal of Neuroradiology 22 (8), 1483–1489.
Whone, A.L., et al., 2003. Plasticity of the nigropallidal pathway in Parkinson's disease. Ann. Neurol. 53 (2), 206–213. https://doi.org/10.1002/ana.10427.
Wu, J., et al., 2020. Longitudinal macro/microstructural alterations of different callosal subsections in Parkinson's Disease using connectivity-based parcellation. Front. Aging Neurosci. 12. https://www.frontiersin.org/articles/10.3389/fnagi.2020.572086. Accessed: 15 August 2023.
Yang, W., et al., 2024. The longitudinal volumetric and shape changes of subcortical nuclei in Parkinson's disease. Sci. Rep. 14 (1), 7494. https://doi.org/10.1038/s41598-024-58187-4.
Yin, K., et al., 2021. Resting-state functional magnetic resonance imaging of the cerebellar vermis in patients with Parkinson's disease and visuospatial disorder. Neurosci. Lett. 760, 136082. https://doi.org/10.1016/j.neulet.2021.136082.
Zeng, L.-L., et al., 2017. Differentiating patients with Parkinson's disease from normal controls using gray matter in the cerebellum. The Cerebellum 16 (1), 151–157. https://doi.org/10.1007/s12311-016-0781-1.
Zhong, Y., et al., 2022. A review on pathology, mechanism, and therapy for cerebellum and tremor in Parkinson's disease. npj Parkinson's Disease 8 (1), 1–9. https://doi.org/10.1038/s41531-022-00347-2.